Zahn, R., Comas, M.C., and Klaus, A. (Eds.), 1999
Proceedings of the Ocean Drilling Program, Scientific Results, Vol. 161

40. MAGNETIC AND MICROFAUNAL CHARACTERIZATION OF LATE QUATERNARY SEDIMENTS FROM THE WESTERN MEDITERRANEAN: INFERENCES ABOUT SAPROPEL FORMATION AND PALEOCEANOGRAPHIC IMPLICATIONS[1]

L. Capotondi[2] and L. Vigliotti[2]

Abstract

Late Quaternary samples collected in the Western Mediterranean Sea at Ocean Drilling Program Leg 161 Sites 974 (Tyrrhenian Sea), 975 (Balearic Basin), and 976 (Alboran Sea) were analyzed for paleoceanographic and paleoclimatic purposes by means of quantitative analysis of planktonic foraminifer and rock-magnetic measurements. The chronostratigraphic framework is based on the comparison between the paleoclimatic curve and oxygen-isotope profiles available for Sites 975 and 976. A poor sedimentary record at Site 974 makes this site unsuitable for the target in the considered time interval. In contrast, a high sedimentation rate allowed a millennial-scale resolution for the last glacial-interglacial cycle (oxygen-isotope stages 1–6) in the Alboran Sea. By combining the organic carbon content, the magnetic properties, and especially the microfaunal assemblage, it has been possible to identify at Site 976 the presence of intervals corresponding to the deposition of sapropels S_1–S_5 in the Eastern Mediterranean Sea. Magnetic parameters show that reductive diagenesis occurs during several time intervals at this site, suggesting that suboxic to anoxic conditions characterize the basin. Sulfur/organic carbon relationships appear in agreement with this observation. In the Balearic Basin (Site 975), the record extends back to oxygen-isotope stage 8. The paleomagnetic record at Site 975 shows the presence of the Blake event, which occurred between the oxygen-isotope substages 5d–5e, as observed in eastern Mediterranean cores by Tucholka et al. (1987).

INTRODUCTION

During Leg 161 a transect of six sites was drilled in the western Mediterranean with the purpose of reconstructing the paleoceanographic and tectonic history of this key area of the basin (Fig. 1). The paleoceanographic target concentrated on the Atlantic-Mediterranean water exchange with a focus on periods of sapropel formation. Sapropels are dark, organic-rich (>2% TOC) layers well known in the eastern Mediterranean (Olausson, 1961; Thunell et al., 1977; Kidd et al., 1978; Cita and Grignani, 1982). Timing of sapropel deposition results independently of climatic conditions (glacial or interglacial intervals) and has been related to astronomical parameters (Hilgen, 1991; Rossignol-Strick, 1985; Lourens et al., 1996). Their occurrence has been interpreted as a response to oceanographic and biogeochemical change: water column stratification leading to bottom water stagnation and/or enhanced productivity (Vergnaud-Grazzini et al., 1977; Thunell et al., 1977; Rossignol-Strick, 1983; Calvert, 1983). Recent micropaleontological (planktonic and benthic assemblages) and geochemical (oxygen and carbon-stable isotope) investigations have shown that, at least during the late Quaternary, organic-rich layers were deposited in the Western Mediterranean Sea (Muerdter 1984; Thunell et al. 1990; Emeis et al., 1991).

Magnetic parameters are extremely sensitive to the anoxic conditions such as those existing at the time of sapropel formation. Several studies show that under suboxic-anoxic environments the deep-sea sediments undergo early diagenesis and lose their original pattern of rock magnetic parameters. Vigliotti (1997) has shown that sapropel-like organic-rich layers recovered in the Japan Sea are characterized by distinctive features such as decrease in concentration of ferrimagnetic minerals, increase in magnetic grain size and coercivity of the remanence, and changes in the magnetic mineralogy with authigenic formation of iron sulfides, such as pyrrothite and/or greigite. Therefore, these layers yield distinctive magnetic features that can be easily identified in magnetic properties profiles.

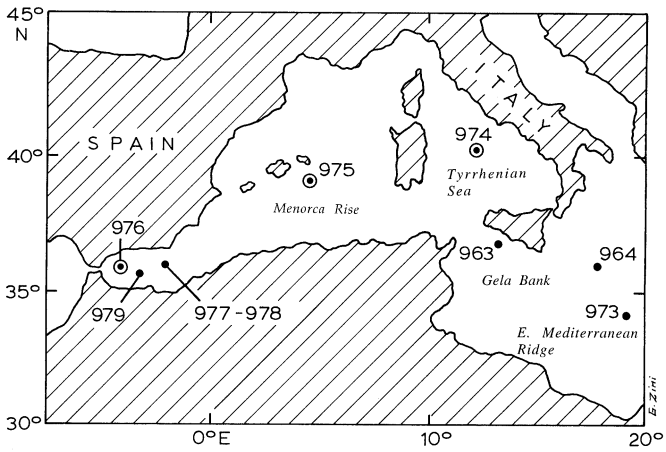

Figure 1. Location of ODP sites drilled in the western Mediterranean during Legs 160 and 161. Circles mark the sites studied in this work.

The aim of this study is to reconstruct the paleoceanographic history of the western Mediterranean during the late Quaternary by comparing the magnetic properties of the sediments with the paleoclimatic record indicated by microfossil analysis. Particular attention will be given to the possible occurrence of the sapropel layers in the westernmost part of the Mediterranean Sea. Rock-magnetic properties and planktonic foraminifer distribution are effective tools for reconstructing the paleoenvironmental record of deep-sea sediments and should be able to test the environmental conditions leading to the sapropel deposition.

A growing number of studies show that variations in the magnetic minerals within deep-sea sediments can be related to paleoceanographic and paleoclimatic changes, such as river influx, variations in carbonate content, the source of the detrital input, sea-level changes, aeolian dust concentration, and oxic-anoxic conditions (Kent 1982; Oldfield and Robinson, 1985; Robinson, 1986; Bloemendal et al., 1988; Doh et al., 1988; Robinson et al., 1995; Vigliotti, 1997). Changes in the concentration, mineralogy, and grain size of magnetic

[1]Zahn, R., Comas, M.C., and Klaus, A. (Eds.), 1999. *Proc. ODP, Sci. Results,* 161: College Station, TX (Ocean Drilling Program).
[2]Instituto per la Geologia Marina, Via P. Gobetti 101, 40129 Bologna, Italy. Vigliotti: mefo@boigm2.igm.bo.cnr.it

mineral assemblages reflect climatically induced variations within the lithogenic fraction of the sediment.

Planktonic foraminiferal assemblages were analyzed quantitatively, used to characterize variations in surface circulation and sea-surface temperature in the western Mediterranean, and compared with variations in global climate inferred from oxygen isotopes. A combination of proxies, such as magnetic parameters and foraminiferal assemblages, is thus an effective tool for reconstructing the paleoenviromental record of deep-sea sediments.

ANALYTICAL METHODS AND MATERIALS

For this study, we focused our attention on ODP Sites 974, 975, and 976 (Fig. 1). The cores were sampled by inserting plastic boxes of about 7 cm^3 into the split-core sections. At first, we sampled the uppermost 25 m of sediments recovered from each of the three sites. After the preliminary studies, we decided that the existence of a continuous and expanded sedimentary record at Site 976 required additional samplings for Sites 976 and 975. The second sampling focused on obtaining a high resolution in a time interval that included the last full glacial-interglacial cycle (140 ka). In this view, more closely spaced samples were collected in the uppermost 10 m at Site 975 and down to a depth of 45 m at Site 976. In the Tyrrhenian Sea (Site 974), this time interval is very poorly preserved; therefore, we did not collect any further samples. We studied a total of 193 samples: 26 from Site 974, 63 from Site 975, and 104 from Site 976.

To characterize the magnetic mineralogy, detailed magnetic measurements were made to investigate the response of the sediments to a variety of applied magnetic fields. This response is mainly determined by the mineralogy, concentration, and grain-size distribution of the magnetic phases.

The procedure used for the magnetic measurements was as follows:

1. Measurements of the low-field mass-specific magnetic susceptibility (χ) at two different frequencies (0.47 and 4.7 KHz) were made by using a MS2 Bartington susceptibility meter. The difference between the two measurements was used to calculate the frequency dependence of susceptibility (χ_{fd}). This parameter reflects the presence within the sediment of very fine (<0.03 μm for magnetite) ferrimagnetic grains in the superparamagnetic state (SP).
2. Measurements were made of the natural remanent magnetization (NRM) before and after stepwise alternating-field (AF) demagnetization with peak fields ranging between 5 and 90 mT. In general, three steps (10, 20, and 30 mT) of AF demagnetization were applied to the samples and further demagnetizations were applied to samples with higher coercivity and/or directions that changed during the cleaning. The remanence was measured with a Minispin spinner magnetometer.
3. Acquisition of anhysteretic remanent magnetization (ARM) was made by subjecting the samples to an AF field of 100 mT biased by a 0.1 mT direct field, followed by progressive AF demagnetization in three steps (20, 30, and 40 mT). The ARM is expressed as anhysteretic susceptibility (K_{arm}), obtained by dividing the ARM by the strength of the DC field.
4. Acquisition of isothermal remanent magnetization (IRM) was made in steps up to a maximum field of 1 T. The acquired IRM (referred as saturation isothermal remanence [SIRM]) was subsequently demagnetized in three steps (15, 25, and 35 mT) and subjected to a backfield of up to –0.3 T. The latter measurements were used to calculate the coercivity of the remanence (B_{0cr}) and the *S*-ratio ($IRM_{-0.3T}$/SIRM). Furthermore, the difference between the SIRM and the IRM acquired by applying a backfield of –0.3T was used to calculate the HIRM parameter expressed as: ($IRM_{-0.3T}$+SIRM)/2 (Robinson 1986). Low-field "soft" IRM (IRM_{100mT}) was used to approximate the total concentration of remanence-carrying ferrimagnets.

Magnetic remanences are expressed in terms of mass by dividing the results by the weight of the samples. Considering that one of the purposes of our study was to investigate the presence of the sapropels in this part of the Mediterranean, at Sites 975 and 976 we measured typical geochemical parameters that characterize these layers, such as total organic carbon (TOC) and sulfur content (S) together with the

Table 1. Total organic carbon, sulfur content, carbon/nitrogen values, and paleoclimatic values used for the paleoclimatic curve at Site 975.

Depth (mcd)	TOC (%)	S (%)	C/N	Paleoclimatic values	Depth (mcd)	TOC (%)	S (%)	C/N	Paleoclimatic values
0.16	0.27	0.093	3.57	15.45	7.9	0.13	—	1.92	–52.35
0.37	0.21	0.082	3.15	–11.69	7.95	0.15	—	2.32	–33.83
0.5	0.27	0.105	3.81	7.43	8	0.17	—	2.43	–14.94
0.78	0.3	0.076	4.15	–84.17	8.19	0.12	—	1.95	–55.68
1	0.18	0.033	2.82	–98.59	8.35	0.17	—	2.66	–67.98
1.24	0.28	0.089	3.69	–86.05	8.63	0.2	—	3.37	–40.37
1.35	0.26	0.064	3.79	–70.35	8.85	0.14	0.002	2.35	10.37
1.6	0.3	0.017	4.55	–71.87	9.15	0.14	—	2.1	7.14
1.8	0.24	0.018	3.91	–76.1	9.42	0.27	—	3.68	–5.9
2	0.23	0.045	3.79	–95.49	9.55	1.23	0.281	7.78	16.03
2.2	0.21	0.014	3.39	–97.27	9.65	0.43	—	4.79	–14.55
2.4	0.23	0.062	3.64	–96.73	10.13	0.29	—	4.39	–91.11
2.65	0.18	0.009	2.9	–98.2	10.65	0.31	—	4.71	–85.64
2.85	0.26	—	4.41	–89.38	10.95	0.32	—	4.49	–91.64
3.45	0.26	—	4.1	–92.51	11.85	0.24	—	3.92	–93.72
3.85	0.21	0.026	3.29	–69.36	12.45	0.19	—	3.17	–99.63
3.93	0.19	0.051	3	–88.73	13.91	0.27	0.028	4.15	–67.73
4.08	0.21	—	3.48	–76.59	15.45	0.33	0.035	4.22	–85.65
4.44	0.32	0.017	4.31	–46.8	15.81	1.02	0.561	8.11	–82.46
4.71	0.18	0.011	2.85	–91.39	16.2	0.26	0.267	3.4	–58.66
4.95	0.2	—	3.23	–94.32	16.37	0.91	0.49	7.37	–75.46
5.17	0.17	—	2.85	–90.96	17.01	0.18	0.022	2.91	–63.25
5.59	0.18	—	2.95	–86.44	17.84	1.55	0.356	9.27	10.82
5.85	0.21	0.019	3.36	–83.41	17.96	0.25	0.013	3.44	–26.49
5.99	0.19	0.011	3.1	–47.94	18.89	0.2	0.077	2.69	–56.92
6.19	0.19	—	2.89	–50.37	19.4	0.32	0.025	4.31	–78.29
6.45	0.16	0.031	2.59	–49.36	20	0.17	—	3.17	–46.68
6.63	0.16	—	2.38	–73.04	20.46	0.76	0.449	6.7	26.65
6.89	0.21	—	3.47	–92.49	20.5	0.27	0.056	3.65	–25.71
7.05	0.22	—	3.64	–66.87	21.5	0.25	0.015	3.45	–64.56
7.35	0.14	—	2.52	–56.61	22.4	0.3	—	4.04	–73.06
7.65	0.14	—	2.72	–52.78					

Note: — = no data available.

Table 2. Total organic carbon, sulfur content, carbon/nitrogen values, and paleoclimatic values used for the paleoclimatic curve at Site 976.

Depth (mbsf)	TOC (%)	S%	C/N	Paleoclimatic values	Depth (mbsf)	TOC (%)	S (%)	C/N	Paleoclimatic values
0.2	0.73	0.04	5.01	–26.87	18.38	0.65	0.5	5.52	–93.26
0.5	0.72	—	—	–28.69	19.48	0.84	0.34	5.86	–74.75
0.7	0.72	0.14	4.39	–13.48	19.88	1.15	0.48	6.83	–83.17
1.07	0.67	0.13	5.22	–22.38	20.1	1.14	0.39	6.98	–78.67
1.32	0.66	0.23	5.1	–22.02	20.99	1.06	0.28	6.41	–86
1.6	0.65	0.21	6.34	–4.16	21.57	0.68	0.47	5.41	–93.62
2.1	0.61	0.1	5.43	–26.52	21.97	0.61	0.24	5.2	–92.74
2.5	0.81	0.33	6.09	–56.94	22.7	0.73	0.25	5.6	–74.6
2.82	0.85	0.35	6.46	–56.57	23.1	0.63	0.4	4.88	–67.36
3.07	0.74	0.26	5.55	–71.6	23.5	0.57	0.19	4.84	–97.77
3.3	0.73	0.39	6.12	–77.1	24	0.49	0.2	4.67	–97.09
3.55	0.73	0.39	5.73	–79.52	24.3	0.51	0.26	4.9	–89.4
3.8	0.87	0.52	6.71	–94.1	24.6	0.44	0.19	4.48	–81.24
3.97	0.99	0.62	7.26	–94.55	24.9	0.39	0.29	4.02	–90.65
4.37	0.87	0.47	6.46	–72.67	25.14	0.36	0.11	4.31	–89.46
4.66	0.85	0.42	6.7	–76.82	25.5	0.42	0.12	4.79	–90.18
4.9	0.77	0.5	6.23	–79.67	26.06	0.73	0.22	6.03	–83.65
5.16	0.73	0.39	5.92	–75.37	26.4	0.85	0.31	6.58	–87.94
5.57	0.63	0.46	5.69	–92.95	26.8	0.68	0.32	6.38	–94.07
5.68	0.64	0.25	5.7	–93.5	27.56	0.79	0.22	5.67	–70.87
6.11	0.52	0.47	5.9	–96.23	28.1	0.69	0.3	6.03	–69.45
6.5	0.56	0.25	6.05	–87.24	29.09	0.7	0.2	5.97	–62.28
6.72	0.5	0.2	5.42	–90.24	29.42	0.56	0.23	5.34	–50.55
7.02	0.56	0.2	5.68	–91.01	29.71	0.58	0.21	5.43	–51.13
7.3	0.52	0.1	5.76	–94.61	30.34	0.59	0.27	5.45	–61.17
8.13	0.49	0.17	5.1	–91.04	30.86	0.38	0.14	4.32	–85.21
8.47	0.57	0.11	6.11	–97.62	31.17	0.53	0.17	5.55	–89.81
8.53	0.52	0.12	5.5	–96.4	31.57	0.69	0.09	6.04	–83.41
8.9	0.48	0.09	4.92	–97.17	32.12	0.79	0.43	6.8	–75.63
9.09	0.45	0.2	4.43	–91.42	32.55	0.75	0.5	6.53	–77.78
9.5	0.57	0.22	4.86	–88.4	33.05	0.72	0.12	6.55	–71.93
9.55	0.49	0.14	4.66	–93.9	33.76	0.71	0.23	6.16	–66.97
10.1	0.51	0.48	4.34	–96.38	34.18	0.66	—	6.28	–67.99
10.6	0.5	—	4.16	–91.67	34.6	0.65	0.28	5.93	–61.39
11.5	0.74	0.22	5.13	–82.21	34.7	0.49	0.18	4.96	–56.83
11.8	0.65	0.34	4.91	–79.72	35.5	0.62	0.19	5.32	–68.56
12.1	0.63	0.39	5.12	–93.84	36.1	0.45	0.17	4.57	–81.78
12.88	0.79	0.59	4.95	–85.39	36.88	0.56	0.05	5.15	–76.73
13.39	0.62	0.63	4.47	–76.65	37.75	0.56	0.43	5.4	–62.28
13.63	0.63	0.22	5.23	–96.79	38.32	0.47	0.07	4.71	–39.44
13.91	0.97	0.63	5.85	–78.94	38.65	0.49	—	4.81	–7.94
14.41	0.94	0.55	6.09	–80.28	39.1	0.47	—	4.72	33.72
14.72	0.78	0.29	5.03	–83.41	39.58	0.51	0.16	4.32	6.46
14.86	0.82	0.4	6.37	–78.82	40.34	0.49	0.22	3.89	–48.37
15.2	0.58	0.28	4.99	–92.1	40.7	0.79	0.47	6.41	–88.84
15.23	0.46	0	4.19	–97.33	41.14	0.88	0.47	6.84	–85.94
15.6	0.76	0.23	5.74	–83.46	41.74	0.64	0.38	5.74	–94.05
16.26	0.86	0.31	6.15	–84.78	42.13	0.42	0.16	4.64	–97.03
16.57	0.79	0.33	5.61	–72.4	42.64	0.63	0.13	5.93	–66.67
17.1	0.93	0.43	6.07	–82.42	43.36	0.48	0.21	5.2	–77.74
17.63	1.02	0.26	6.36	–68.55	43.69	0.48	—	—	–73.54
18.02	0.7	0.3	5.15	–60.34	44.18	0.42	0.16	4.98	–92.83

Note: — = no data available.

total nitrogen (N) content. They were measured by using a Carlo Erba CHN analyzer. The values, expressed as percentages, are given in Tables 1 and 2, along with the paleoclimatic values.

The samples for the microfaunal analyses were dried at 60°C, washed and sieved through 63- and 125-µm sieves to separate two size fractions: one >125 µm and the other between 63 and 125 µm. Both these sizes were used for qualitative analyses of the foraminifer microfauna. Quantitative analyses were conducted on the fraction above 125 µm for the samples collected at Sites 975 and 976, and above 63 µm at Hole 974B. For each sample, more than 300 planktonic specimens, which were separated with a microsplitter, were identified and counted. Some species, such as sinistral and dextral coiling of *Globorotalia truncatulinoides* and *Neogloboquadrina pachyderma*, were counted separately. We have also differentiated the morphotypes of *Globigerinoides ruber* (*G. ruber* var. *rosea* and *alba*), whereas *Globigerinoides tenellus* and *Globigerina rubescens* were counted all together.

The paleoclimatic curve was computed as the sum of the percentages of warm-water indicators (positive values) and the cold-water indicators (negative values) following the method proposed by Cita et al. (1977). Based on distribution patterns of living planktonic foraminifers in the Mediterranean sea (Cifelli, 1974; Thunnell, 1978; De Castro Coppa et al., 1980; Pujol and Vergnaud-Grazzini, 1995) we have considered warm-water species to be *Globigerinoides ruber, G. gomitulus, G. elongatus, Globigerinoides tenellus, G. sacculifer, O. universa, Hastigerina pelagica, Hastigerina siphonifera,* and *Globigerina rubescens*. Cold-water species are represented by *Globigerina bulloides, T. quinqueloba, Globorotalia scitula, Neogloboquadrina pachyderma* (d. and s.), and *Globigerina glutinata.*

CHRONOSTRATIGRAPHIC FRAMEWORK

A detailed chronological framework for the sediments studied has been developed by means of micropaleontological analysis, nannoplankton data (Comas, Zahn, Klaus, et al., 1996) paleomagnetic data, and oxygen-isotope stratigraphy available from Site 975 (Pierre et al., Chap. 38, this volume) and Site 976 (von Grafenstein et al., Chap 37, this volume). The paleomagnetic data show that all the samples belong to the Brunhes Chron (0–0.78 Ma).

As shown by several authors (Cita et al., 1977; Vergnaud-Grazzini et al., 1977; Capotondi et al., 1994) the paleoclimatic curve can approximate in good detail the oxygen-isotope records for the time interval considered. A comparison between the shape of the $\delta^{18}O$ curve with the fluctuations of the paleoclimatic curve indicates that they yield similar trends. Positive and negative peaks in the planktonic foraminifer record correspond to interglacial and glacial isotope stag-

es. Based on these considerations, we have tuned the ages of the sediments to the oxygen-isotope stages of Martinson et al. (1987).

Samples from Hole 974B represent the longest record with poor time constraints. On-board data of calcareous nannoplankton record the first occurrence (FO) of *E. huxleyi* (NN21A; 0.26 Ma) at the bottom of the first core (161-974B-1H-CC; 6.5 mbsf) and the last appearance datum (LAD) of *P. lacunosa* (NN20; 0.46 Ma) at about 11.61 mbsf. A somewhat speculative interpretation of the stratigraphic framework, which is based on a comparison with ODP Site 652, in the Tyrrhenian Sea (Vergnaud-Grazzini et al., 1990), suggests that our last sample belongs to oxygen-isotope stage 15 (0.565–0.62 Ma; according to Imbrie et al., 1984).

The age of the sediments studied from Site 975 appear well constrained by the first occurrence (FO) of the *E. huxleyi* (0.26 Ma) that has been recognized at a depth of about 21.67 m (Comas, Zahn, Klaus, et al., 1996), which means very close to our last sample (22.4 mcd). Further constraints in the age of the uppermost six isotope stages have been obtained by comparison with the data of a previously studied core (Bal84-2) recovered in the same area (Table 3; Capotondi et al., 1987).

At this site, the paleomagnetic data exhibit a short interval of reversed polarity between 7.77 and 8.35 mcd. As discussed in the paragraph about the NRM of the sediments, the stratigraphic position of this interval suggests that it represents the Blake Event, which has been observed at several sites around the world and has been dated in the Mediterranean Sea between 117 and 123 ka (Tucholka et al.,1987).

A closely spaced sampling of up to 4 samples per meter was performed at Site 976. The $\delta^{18}O$ profile exhibits a good agreement with the record observed at Site 659 in the Equatorial Atlantic and suggest that our sampling represents oxygen-isotope stages 1–6 (von Grafenstein et al. Chap. 37, this volume). The paleoclimatic curve obtained for this site is in agreement with this interpretation, so the sampling spans about 150 k.y. For the last glacial time interval, a detailed time control was obtained on the basis of the ecozones method described by Pujol and Vergnaud-Grazzini (1989). The identified peaks in frequency of *N. pachyderma* (P1, P2, P3, P4), *G. quinqueloba* (Q1, Q2), and *G. bulloides* (B1, B0) have been correlated with the events dated by these authors, and they represent eight well-defined time-control points (see Table 4) for the Last Glacial Maximum (LGM)–Holocene interval.

RESULTS

Natural Remanent Magnetization (NRM)

The NRM of all the samples was studied by stepwise (AF) demagnetization of variable peak field, according to the coercivity of the sediments. The intensity of magnetization is different from site to site with the highest value observed at Site 974 and lowest value measured at Site 976. This reflects the different source of the magnetic minerals between the sites. As shown in Figure 2, the magnetic inclinations are almost exclusively positive, which indicates that all the samples belong to the Brunhes Chron. A couple of exceptions have been observed, showing negative inclinations: a small interval between 7.9 and 8.4 mcd at Site 975, and a couple of samples at ~14 m depth at Site 976. The former is clear after the AF cleaning. This observation gives credit to the event as representative of a primary magnetization. The stratigraphic position, in particular, strongly supports a correlation with the Blake Event. This event is documented by full-reverse field directions at several sites around the world. By correlation with the oxygen-isotope stratigraphy the event has been dated in the Mediterranean between 117 and 123 ka by Tucholka et al. (1987). This age is well in agreement with the Chinese loess record that shows the Blake Event just above the Eemian interglacial (Fang et al., 1997). The stratigraphic position of the observed reverse interval is coincident with the beginning of the reversal at about 123 ka while

Table 3. Biostratigraphic and isotopic points used for the reconstruction of the sedimentation rate at Site 975.

Depth (mcd)	Age (k.y.)	Remarks
0.5	8.5	Planktonic microfaunal assemblage
1.32	18.0	Last Glacial Maximum evidenced by planktonic microfaunal assemblage
2.05	24.11	3.0 oxygen-isotope stage
4.57	58.96	4.0 oxygen-isotope stage
6.45	103.29	5c3 oxygen-isotope substage
7.05	110.79	5d oxygen-isotope substage
8	122.56	5e1oxygen-isotope substage
8.85	123.82	5e3 oxygen-isotope substage
9.55	125.9	5e5 oxygen-isotope substage
9.89	129.8	6.0 oxygen-isotope stage
17.42	189.6	7.0 oxygen-isotope stage
21.0	244.18	8.0 oxygen-isotope stage

Note: The planktonic microfaunal assemblage is correlated with Capotondi et al. (1987). Age for the isotope stages and substages are derived from the chronostratigraphy of Martinson et al. (1987).

Table 4. Biostratigraphic and isotopic points used for the reconstruction of the sedimentation rate at Site 976.

Depth (mbsf)	Age (k.y.)	Remarks
1.32	4.0	B0 biological event
2.50	8.3	P1 biological event
3.30	9.0	Q1 biological event
3.80	10.7	P2 biological event
5.16	13.0	B1 biological event
5.57	14.5	P3 biological event
6.11	15.0	Q2 biological event
6.72	16.0	P4 biological event
7.5	18.0	Last Glacial Maximum evidenced by planktonic microfaunal assemblage
11.50	27	3.1 oxygen-isotope substage
23.30	58.96	4.0 oxygen-isotope stage
27.16	73.91	5.0 oxygen-isotope stage
31.17	90.95	5b oxygen-isotope substage
32.07	96.21	5c1 oxygen-isotope substage
34.70	103.29	5c3 oxygen-isotope substage
36.10	110.79	5d oxygen-isotope substage
39.10	123.8	5e oxygen-isotope substage
40.70	129.8	6.0 oxygen-isotope stage

Note: Biological events ages are according Pujol and Vergnaud-Grazzini (1989). Ages for the isotope stages and substages are derived from the chronostratigraphy of Martinson et al. (1987).

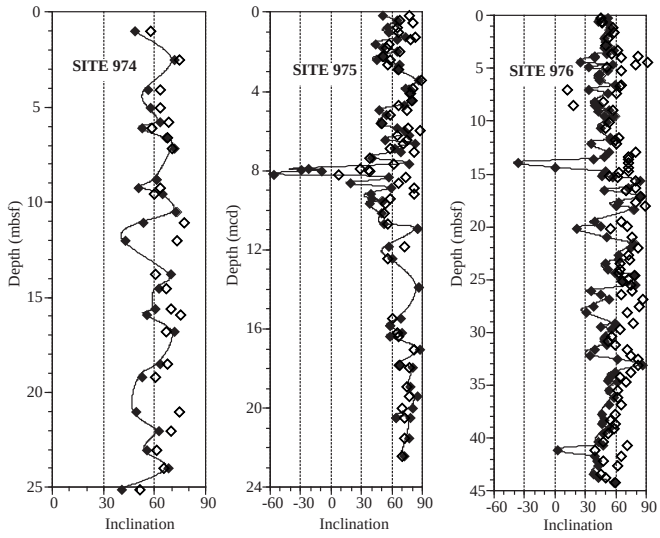

Figure 2. Inclination values recorded at Sites 974, 975, and 976. Open symbols indicate NRM values; solid symbols show the inclinations after AF cleaning.

the length appears a little bit shorter. On the basis of the sedimentation rate, the event appears to have ended at about 119 ka. It occurs in the Core 161-975B-2H, just one meter above the sapropel S_5, which is known to have been deposited during the Eemian at about 124 ka (astronomical age; Lourens et al., 1996). Moreover, the detailed oxygen-isotope stratigraphy available for this interval (Pierre et al., Chap. 38, this volume), assigns this event midway between the substages 5d and 5e, exactly in the same position recognized by Tucholka et al. (1987) in eastern Mediterranean cores.

In spite of the high sedimentation rate, this event has not been observed at Site 976. Heavy remagnetization induced by the drilling was documented for the sediments recovered during Leg 161 (Comas, Zahn, Klaus, et al., 1996), so it is possible that the strong overprint masks the event. The down-core plot of the magnetic inclinations shows, after cleaning, two samples with negative inclinations at about 14 m of depth (Fig. 2). At this stage they cannot be considered unequivocally representative of a geomagnetic reversal; however, if they do represent a true event, the stratigraphic position within oxygen-isotope stage 3 may be compatible with the Laschamp excursion that has been reported in literature with ages scattered between 32 and 50 ka (Nowaczyk et al., 1994).

Site 974

Site 974 is located in the central Tyrrhenian Sea on the western side of the De Marchi Seamount at 3668 m water depth, ~300 m from ODP Site 652. Twenty-six samples were studied from the uppermost 25 m of sediments, which consist of hemipelagic deposits, mainly nannofossil-rich clay. Volcanoclastic layers occur throughout the cores and several samples exhibit a size fraction of only <40–63 µm, attesting that fine-grained turbidites are frequent in these sediments (Fig. 3). The presence of fine-grained turbidites, together with a low sedimentation rate (about 5.5 cm/k.y. for the Pleistocene–Holocene; Comas, Zahn, Klaus, et al., 1996) and a possible hiatus in the interval studied, accounts for the poor resolution obtained at this site. Nevertheless, a comparison between the paleoclimatic trend and the oxygen-isotope record obtained at Hole 653A, also in the Tyrrhenian Sea (Vergnaud-Grazzini et al., 1990), allows us to attribute our last sample (161-974B-3H-7, 10–12 cm; 25.12 mbsf) to isotope stage 15 (about 0.65 Ma). The warm-water microfaunal assemblage found at 1 mbsf is a record of the oxygen-isotope substage 5e. The sapropel layer recognized in Sample 161-974B-3H-3, 19–21 cm, could be related to the oxygen-isotope stage 13 (0.478–0.524 Ma, according to Imbrie et al., 1984) and probably corresponds to the sapropel S_{11} or S_{13}.

Rock magnetic parameters measured on the 26 samples collected from Hole 974B do not show any particular trend as can be observed in the susceptibility profile shown in Figure 3. Two peaks in concentration parameters χ, K_{arm}, and SIRM occur at 6.5 and 14.5 mbsf and represent volcanoclastic layers. Interparametric ratios exhibit a narrow range of values, which indicates only minor changes in magnetic grain-size (Fig. 3). The *S*-ratio is above 0.9 in all the samples (Fig. 3) and the coercivity of the remanence (B_{0cr}) is in the range 30–40 mT, indicating that ferrimagnetic minerals (magnetite-type) dominate the magnetic properties.

Site 975

Site 975 was drilled in the Balearic Basin in 2415 m water depth. The interval studied (uppermost 22 m) consists of nannofossil ooze with five well-identified organic-rich layers that correspond to the sapropel S_5–S_9. The total organic carbon content ranges from 0.1% to 1.5% (Table 1), but, in general, is quite low, especially in the uppermost 9 m, which is below 0.3%, the common value for typical deep-sea sediments (McIver, 1975). Only in some of the well-identified sapropel layers do the TOC values exceed 1% (Fig. 4).

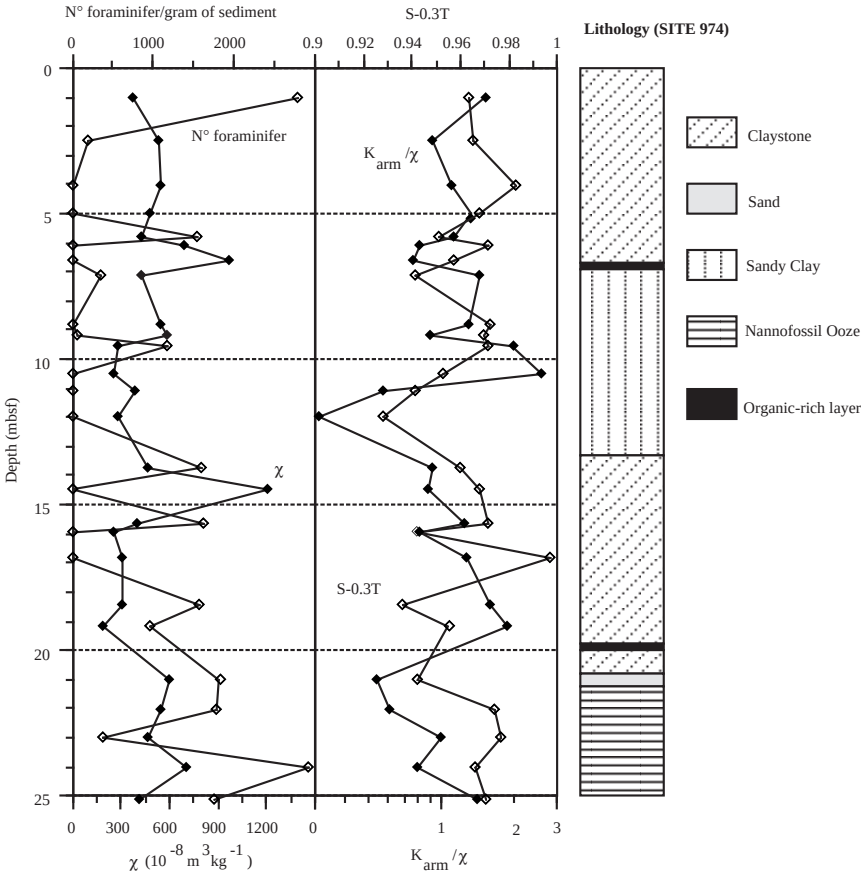

Figure 3. Comparison of planktonic foraminifer abundance vs. magnetic susceptibility and down-core variations of magnetic parameters K_{arm}/χ_χ and *S*-ratio at Site 974.

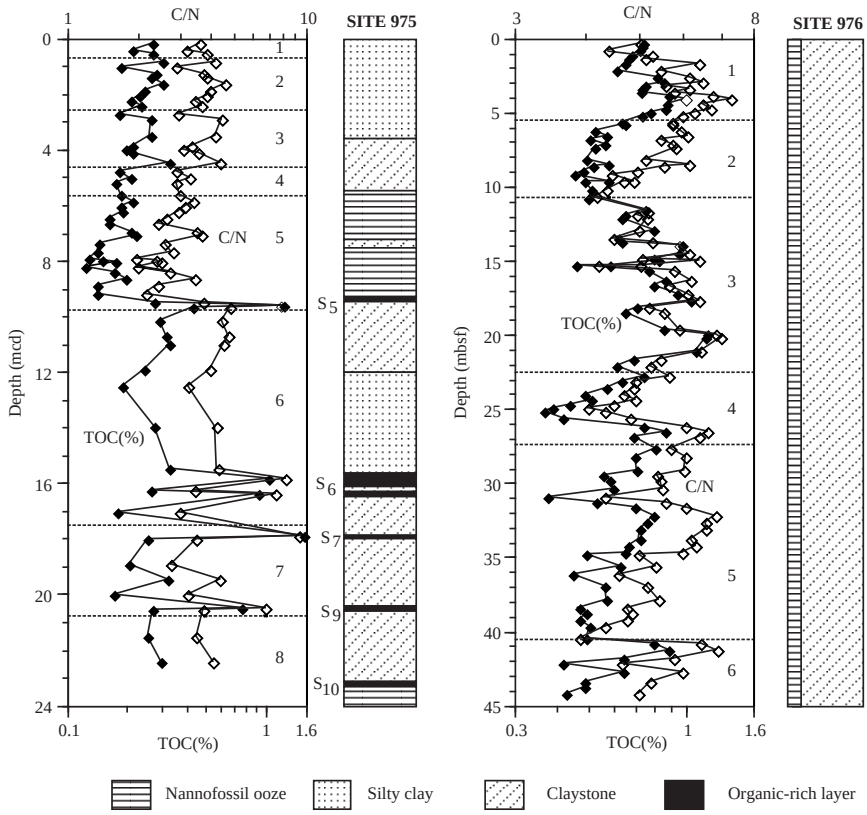

Figure 4. Down-core variations of TOC and carbon/nitrogen values at Sites 975 and 976.

The paleoclimatic trend recognized at Site 975 identifies into eight intervals, which correspond to oxygen-isotope stages 1–8 (Last 260 ka, according to Martinson et al., 1987). The age of stage and substage boundaries is listed in Table 3 and shown in Figure 5.

The bottom of the paleoclimatic curve shows low values associated with a cold assemblage (dominance of *G. quinqueloba*, *G. bulloides*, *G. glutinata*, *N. pachyderma*, and *G. scitula*), which is related to oxygen-isotope stage 8.

Between 21 and 17.42 mcd, the ameliorating climatic conditions are attested to by abundant frequencies in *G. ruber* and *G. inflata*. This interval corresponds to oxygen-isotope stage 7. Positive fluctuations in the paleoclimatic curve are documented at 20.46 and 17.84 m and are characterized by the presence of a warm planktonic foraminiferal assemblage similar to the microfauna recognized in the sapropels S_9 and S_7 found in the Eastern Mediterranean Sea (Cita et al., 1982). The negative interval around 19.4 m contains a higher percentage of *N. dutertrei* and corresponds to the stagnant phase related to the deposition of sapropel S_8.

Following this interval, the paleoclimatic values vary between –60 and –100 in correspondence to oxygen-isotope stage 6. At 15.81 and 16.37 m, a peak in the frequencies of *N. dutertrei* and *G. bulloides* allow us to recognize the two phases that characterize sapropel S_6.

The rapid transition between cold and warm conditions at 9.89 m corresponds to the beginning of the isotope stage 5. A significant and rapid cooling is documented by three samples between 8.63 and 8.19 m. This event abruptly breaks the gradual decrease of temperature between substage 5e1 (8 m) and substage 5d (7.05 m). This interpretation is supported by the Blake Event recorded at 8.19 m (Fig. 2).

Above 6 m of depth, a drastic decrease in the paleoclimatic values suggests a rapid transition to oxygen-isotope stage 4. A positive peak observed at 4.44 m contains a sapropel faunal assemblage that we interpret as time-equivalent to the S_2 deposition in the eastern Mediterranean, if this sapropel existed (Vergnaud-Grazzini et al., 1977; Muerdter et al., 1984). A rapid shift occurs at the transition from the Last Glacial Maximum (1.32 m) to the Holocene.

The magnetic parameters measured on the 63 samples collected from the cores recovered in the Menorca Rise yield well-defined trends that fit very well with the paleoclimatic record observed at Site 975 (Fig. 6). A very good correlation exists between the K_{ARM} profile and the paleoclimatic curve, which suggests that stable single domain (SSD) grains are somehow related to climate (Fig. 7). Glacial stages are also characterized by larger grain size as well as by higher coercivity and lower *S*-ratio (Fig. 6). The contribution of superparamagnetic (SP) grains, expressed by the χ_{fd} parameter, is higher during the interglacials 1, 5, and 7 and reaches the maximum value in the uppermost three samples, which belong to the Holocene (Fig. 6). Magnetic mineralogy is dominated by ferrimagnetic minerals; however, as shown by the HIRM profile, the contribution of antiferromagnetic minerals (hematite-type) increases during the glacial stages and seems quite significant during isotope stage 2 (Fig. 6).

Three organic-rich layers well identified in the lithology (9.55, 15.81, and 17.84 mcd) and corresponding to sapropels S_5, S_6, and S_7, exhibit a significant decrease in magnetic concentration, whereas Sample 161-975C-3H-5, 56–58 cm (20.46 mcd), corresponding to sapropel S_9, yields a significant content of magnetite. However, the sample is characterized by an increasing magnetic hardness, as suggested by higher value of B_{0cr}.

Site 976

Site 976 is located in 1107 m water depth in the Alboran Sea about 60 km south of the Spanish coast and only 110 km west of the Gibraltar Strait. From an oceanographic point of view, it is very sensitive to the Atlantic-Mediterranean water-mass exchange. The sedimentation rate is high, ranging between 30 and 50 cm/k.y. (Comas, Zahn, Klaus, et al., 1996). The 45 m of sediment studied at Hole 976C is represent-

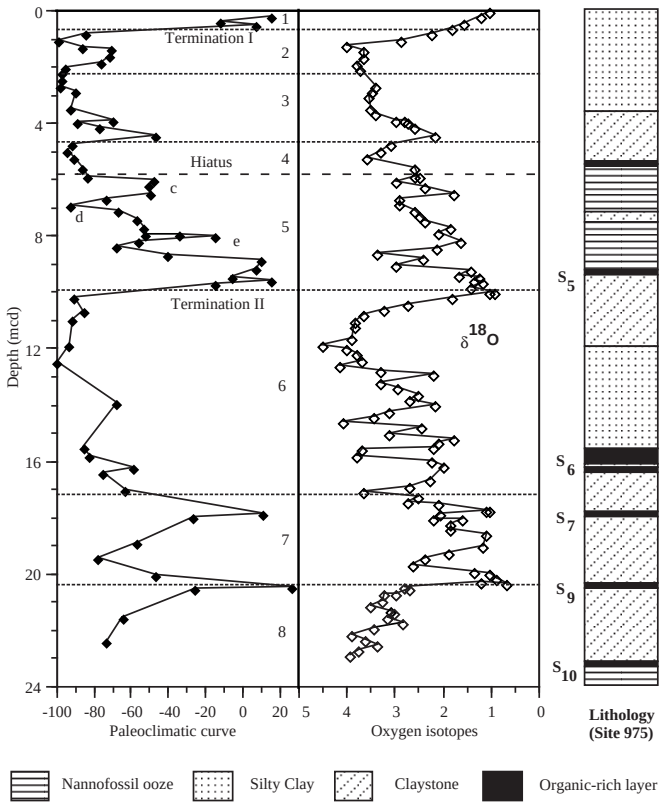

Figure 5. Comparison between the paleoclimatic curve obtained from the planktonic foraminifer assemblage (see text for details) and the oxygen-isotope data (Pierre et al., Chap. 38, this volume) from Site 975. Dotted lines = oxygen-isotope boundaries; dashed line = a hiatus recognized between the oxygen-isotope stages 4 and 5c. Small discrepancies between the foraminifer and oxygen-isotope records are related to the different holes used for the two proxies.

ed by open-marine hemipelagic facies of nannofossil-rich clay without any significant color change. The TOC measured on the samples studied is relatively high with values ranging between 0.35%–1.15%, averaging around 0.6% (Fig. 4; Table 2).

The agreement between the paleoclimatic curve and oxygen-isotope record (Fig. 8) indicates that our record spans the last six isotope stages. The depth and age of stage and substage boundaries are listed in Table 4 and shown in Figure 8.

The lower part of the section investigated shows low values in the paleoclimatic curve, which are related to the oxygen-isotope stage 6, as indicated by the dominance of cold species such as: *N. pachyderma, G. quinqueloba,* and *G. bulloides*. The warming indicated by the occurrence of *G.* ex gr. *ruber, O. universa,* and presence of *G. inflata* (a low percentage) characterizes the glacial/interglacial transition equivalent to the oxygen-isotope stage 6/5 boundary.

Between 40.70 m and 27.16 m the paleoclimatic values are characterized by a predominance of warm assemblages with high-amplitude variations. The major positive climatic cycles are related to oxygen-isotope substages 5e, 5c, and 5a. During these oxygen-isotope substages at 39.1–38.65 m, 34.18–33.05 m and 29.42 m, we have recognized three "sapropel-layer assemblages," corresponding respectively to the time deposition in the Eastern Mediterranean Sea of sapropels S_5, S_4, and S_3 (Cita et al., 1977; Vergnaud-Grazzini et al. 1977). A decrease in the percentage of warm-water species allow us to identify oxygen-isotope cold substages 5d at 36.10 mbsf and 5b at 31.17 mbsf.

The transition between oxygen-isotope stages 5/4 is not straightforward. The paleoclimatic record exhibits an oscillation that cannot be unequivocally associated to the warm or cold stage (Fig. 8). Upon consideration of the sedimentation rate, we regard this swing as a warm oscillation at the base of isotope stage 4. In a speculative way, we can correlate this interval to the interstadial 20 in the GRIP ice core, (Dansgaard, 1993), which corresponds also to the Ognon II warm event at the Gran Pile peat bog in France (Woillard, 1978). Oxygen-isotope stage 4 is characterized by high frequencies of polar species *G. quinqueloba* (peak values 50%–70%) and the dominance of cold indicators such as *G. bulloides, N. pachyderma,* and *G. glutinata*.

The time interval attributed to oxygen-isotope stage 3 shows high frequency climate fluctuations. This time interval is characterized by the presence of *G. inflata* and by marked fluctuations in *N. dutertrei* distribution. An interval with warm species between 20.99 and 20.10 mbsf yields a "sapropel planktonic fauna" that corresponds to an insolation maximum (von Grafenstein et al., Chap. 37, this volume) that would be coeval with the sapropel S_2 in the Eastern Mediterranean, if this sapropel existed. It shows also the highest peak in the TOC profile (Fig. 4). The transition between oxygen-isotope stages 3/2 corresponds to a rapid decrease of *G. inflata* and a general cooling trend. The Last Glacial Maximum (18 ka) is identified at 7.5 mbsf and is characterized by the exclusive presence of cold species *N. pachyderma* (left and right coiling), *G. quinqueloba, G. bulloides, G. glutinata,* and *G. scitula*. The high sampling resolution in the upper part of the core allows us to recognize several well-defined climatic steps discussed in Pujol and Vergnaud-Grazzini (1989) in the same area.

The gradual warming during the deglaciation is characterized by different climatic phases related to the changing hydrological setting, as suggested by diachronous peaks in frequency of *G. bulloides, N. pachyderma,* and *G. quinqueloba*. The cold, short interval between 4.3–3.8 mbsf corresponds to the Younger Dryas event. This correlation is supported by pollen data (Combourieu Nebout et al., Chap. 36, this volume) and also by the finding of a *Malletia* shell in Sample 161-976C-1H-3 80–82 cm (3.8 mbsf). This bivalve protobranch is typical of cold waters and lives today in arctic regions (M. Taviani, pers. comm.).

The warm climatic variation at 2.50–2.82 mbsf shows a sapropel planktonic assemblage, which correlates to sapropel S_1. The planktonic microfaunal association recognized in the uppermost samples is very similar to the present-day assemblage.

Each of the parameters that reflects variations in the magnetic concentration (χ, SIRM, HIRM), shows the highest value in the uppermost 3.5 m of sediments that belong to the Holocene (Fig. 9). This interval is also characterized by peak values (6%–9%) in the frequency dependent susceptibility. A drastic decrease in magnetic concentration together with increasing grain size, peak values in coercivity of the remanence, and minimum in *S*-ratio ($S_{-0.3T}$) distinguish the interval 3.5–5 mbsf (Fig. 9), which includes the Younger Dryas. Similar trends in the magnetic properties are observed throughout the sequence studied. In fact, we have some intervals in which rock-magnetic parameters drop to very low values, with the greatest reduction observed in the case of the K_{ARM} parameter (Fig. 7). These fluctuations coincides with similar trends in the concentration-independent parameters (K_{arm}/χ; SIRM/χ, and ARM/SIRM) and in the *S*-ratio (Fig. 9). The data indicate that intervals corresponding to low-magnetic content are also characterized by a coarsening of the grain size and an increase in the ratio of the goethite/hematite to magnetite. The longest interval showing the above-mentioned characteristics spans most of the oxygen-isotope stage 3, while a primary contribution of ferrimagnetic minerals occurs in samples deposited during oxygen-isotope stage 5 (Fig. 7).

These characteristics are typical of sediments that have undergone a significant diagenetic loss of magnetite. Selective dissolution of

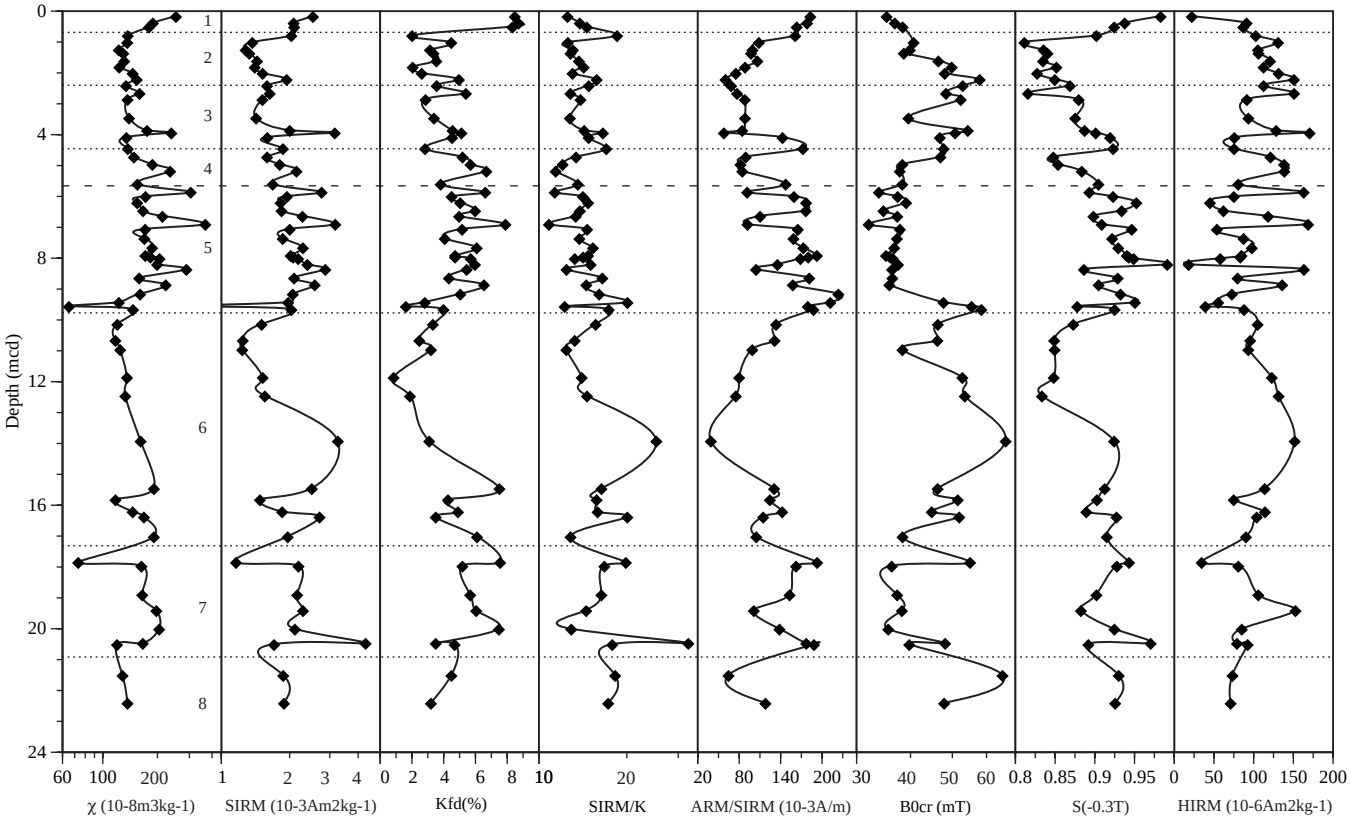

Figure 6. Downcore variations of magnetic parameters and interparametric ratios measured on samples from Site 975. Dotted lines = the boundaries between the oxygen-isotope stages, indicated by the small numbers in the left column.

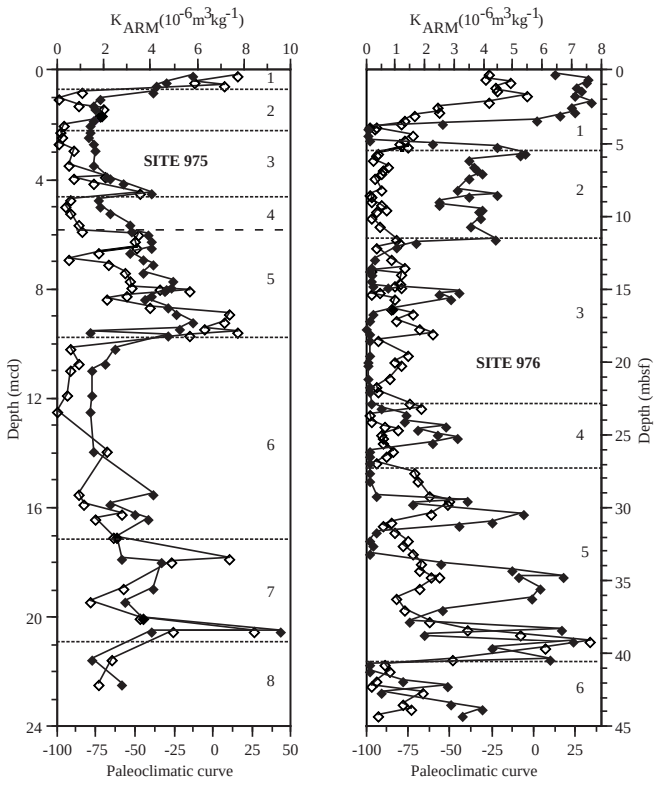

Figure 7. Downcore variations of magnetic parameter K_{ARM} along with the paleoclimatic curves obtained at Sites 975 and 976.

magnetite has been recognized in several suboxic/anoxic environments all around the world (e.g., Karlin and Levi, 1983; Canfield and Berner, 1987; Karlin, 1990; Tarduno and Wilkison, 1996) and seems to have been active also in the Alboran Sea. The organic-matter content of these sediments is higher than in deep-sea sediments and pyrite has been observed in several samples, which implies that sulfate reduction is an active process. Organic-carbon–rich sediments can be obtained by either an increasing organic productivity or an increased preservation of the organic matter under oxygen-deficient deep-water conditions (Stein, 1990). In order to decide which of these mechanisms is responsible for the organic matter accumulation, the relationship between the organic carbon and the sulfur content may be helpful (Leventhal, 1983; Berner, 1984). According to these authors, in normal-marine, fine-grained, detrital sediments, the mean C/S ratio is 2.8. A plot of the TOC vs. total S (Fig. 10) shows that anoxic conditions prevailed during the deposition of several samples. In comparison, Site 975 exhibits anoxic conditions only during the deposition of sapropel layers.

DISCUSSION

A good paleoclimatic record has been obtained from the planktonic foraminiferal assemblage of both Sites 975 and 976 in the Western Mediterranean. The close correspondence between paleoclimatic trends and the oxygen-isotope record suggests a strong control of the temperature in faunal planktonic distributions. Also, rock magnetic parameters show a correlation with the paleoclimatic record, indicating that climate exerts a major role on the magnetic properties of these sediments.

By using the ages of well-identified points (bioevents, oxygen-isotope stage boundaries, and climatic events, Blake Event), it has

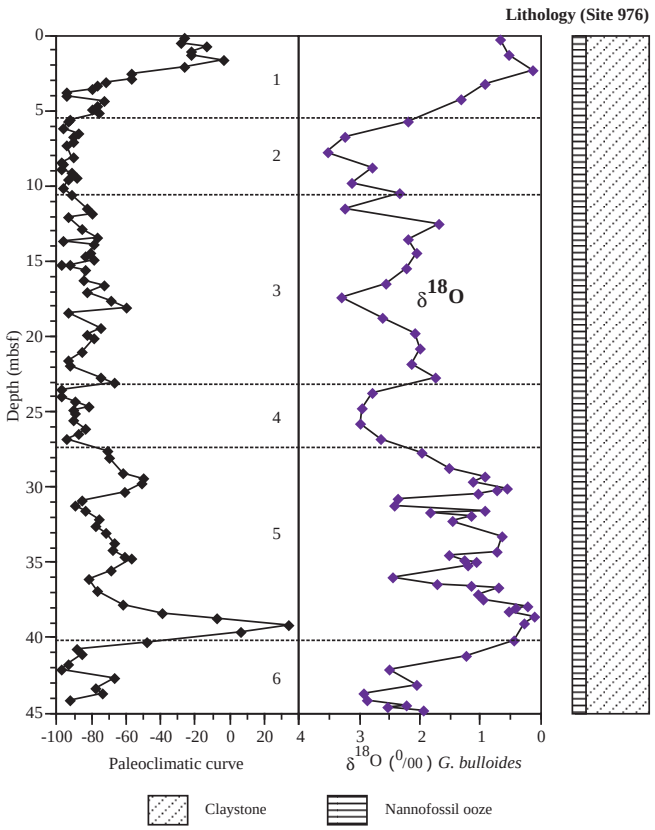

Figure 8. Comparison between the paleoclimatic curve obtained from the planktonic foraminifer assemblage (see text for details) and the oxygen-isotope data (von Grafenstein et al., Chap. 37, this volume) from Site 976. Dashed lines = oxygen-isotope boundaries. Small discrepancies between the foraminifer and oxygen-isotope record are related to the different holes used for the two proxies.

been possible to reconstruct a detailed sedimentation rate for these sites (Fig. 11). A significant difference exists between the Balearic Basin and the Alboran Sea, which reflects the different amount in the supply of terrigenous material between the two sites. In the Balearic Basin we have a quite constant sedimentation rate of about 7 cm/k.y. from the Holocene back to oxygen-isotope stage 4. Corresponding to the beginning of oxygen-isotope stage 5, there is an apparent decrease in the sedimentation rate that is a result of a gap recognized between the end of the oxygen-isotope stage 4 and substage 5c (Fig. 5). In particular, the presence of a "sapropel-like" planktonic foraminiferal assemblage corresponding to the end of this hiatus suggests that the missing record spans the time interval beginning at the end of the oxygen-isotope stage 4 (about 73.9 k.y.; Martinson et al., 1987) and the sapropel S_4 (102 k.y.; Lourens et al., 1996).

It is noteworthy that a significant increase in the sedimentation rate occurs during the Eemian (substage 5e). At Site 975 the sediments also exhibit a low organic carbon content (Fig. 4) that above 9.5 m of depth is almost constantly below the values recorded in normal open-marine environments (0.3%; Stein 1991).

At Site 976, the sedimentation rate ranges between 34 and 50 cm/k.y. Higher sedimentation rates occur for the last two oxygen-isotope stages. The total organic carbon measured at this site exceeded the values of 0.5% in most of the samples (Fig. 4), which is distinctly higher than those observed in open-marine environments. The carbon/nitrogen ratio (C/N) is quite constant with values ranging between 4 and 11, indicating the predominance of marine organic matter in the Alboran Sea (Fig. 4). Furthermore, the organic-carbon/sulfur ratio indicates that several intervals were deposited during anoxic conditions.

The TOC profile exhibits a trend that appears correlated with the climatic variations. High/low organic carbon content corresponds to warm/cold periods (Fig. 4). Nevertheless a couple of intervals show a different feature. In fact, the Termination I and II are both characterized by peaks in the TOC values, whereas the Eemian substage yields quite low values. The observed oscillations cannot be related to changes in the sedimentation rate, which would enhance the preservation of the organic matter (Stein, 1991). Therefore, the variations in the organic matter content correspond to changes in the primary productivity. A parallelism between the TOC values and the *N. dutertrei* distribution supports this observation (Fig. 12). The high abundance of this species reflects the presence of a Deep Chlorophyll Maximum (DCM; Thunell, 1979; Fairbanks et al., 1982; Rohling and Gieskes, 1989; Pujol and Vergnaud-Grazzini, 1995).

It is noteworthy that both Termination I (including the Younger Dryas) and II are characterized by peak values in the C/N ratio with values that suggest a possible increasing contribution of terrestrial organic matter during these periods (Fig. 4).

Possible Sources of the Magnetic Minerals

The fluctuations in magnetic concentration and grain size reflect changes in the types of magnetic minerals supplied to the sediments, as well as the nature of depositional paleoenvironments. In general, the magnetic concentration is low in biogenic sediments and high in terrigenous materials. Exceptions to this feature often occur in marine sediments because (1) dilution by other sedimentary components; (2) increasing distance from sources of magnetic minerals; (3) diagenetic processes; and (4) authigenic formation of bacterial magnetite.

The magnetic properties measured in the samples from Site 974, 975, and 976 exhibit differences that are related to either different sources of the magnetic minerals or to different environmental conditions of the basins. At all the sites the dominant magnetic mineral is magnetite. *S*-ratio values suggest that a relative importance of antiferromagnetic minerals occurs only during the glacial stages at Site 975 and in the intervals of reductive diagenesis observed at Site 976. In the former site, the antiferromagnetic minerals present within the sediments are probably related to an increasing contribution of the aeolian fraction (Saharan dust) during these cold stages. The highest concentration of magnetic minerals occurs in the Tyrrhenian Sea and the possible source of the relatively coarse-grained magnetite in this area can be identified with the volcanic provinces of central and southern Italy (McCoy and Cornell, 1990). In the Balearic Basin (Site 975), the K_{ARM} profile exhibits a correlation with glacial and interglacial stages (Fig. 7), which would suggest that bacterial magnetite is the most likely source for these sediments. In the Alboran Sea, the ferrimagnetic minerals within the sediments are likely supplied by terrigenous material. Site 976 is located in shallow water with respect to the other sites, where very probably the source area for the magnetic materials lies in the southern Spanish coast. These observations are supported by the plot of ARM/SIRM vs. IRM_{100}/SIRM shown in Figure 13. This plot reflects the contribution of SSD (high ARM/SIRM values) with respect to the ferrimagnetic:antiferromagnetic ratio (increasing values of IRM_{100}/SIRM). The samples from Site 975 exhibit the highest ARM/SIRM value within a range that includes the values obtained for deep-sea sediments considered to have magnetic properties dominated by bacterial magnetosomes (Oldfield, 1994). An unequivocal interpretation of these data would require microscope observations of the typical structure of bacterial magnetite and will be the subject of a future investigation.

At Site 976 concentration (χ, SIRM, ARM), grain-size (K_{arm}/χ, SIRM/χ, ARM/SIRM) and coercivity (*S*-ratio, B_{0cr}) parameters show a similar trend, implying that they are controlled by a unique factor. This factor is a process of reductive diagenesis related to bacterial degradation of organic matter. The organic-carbon/sulfur relationship clearly shows the difference between this site and the site drilled in the Balearic Basin (Fig. 10).

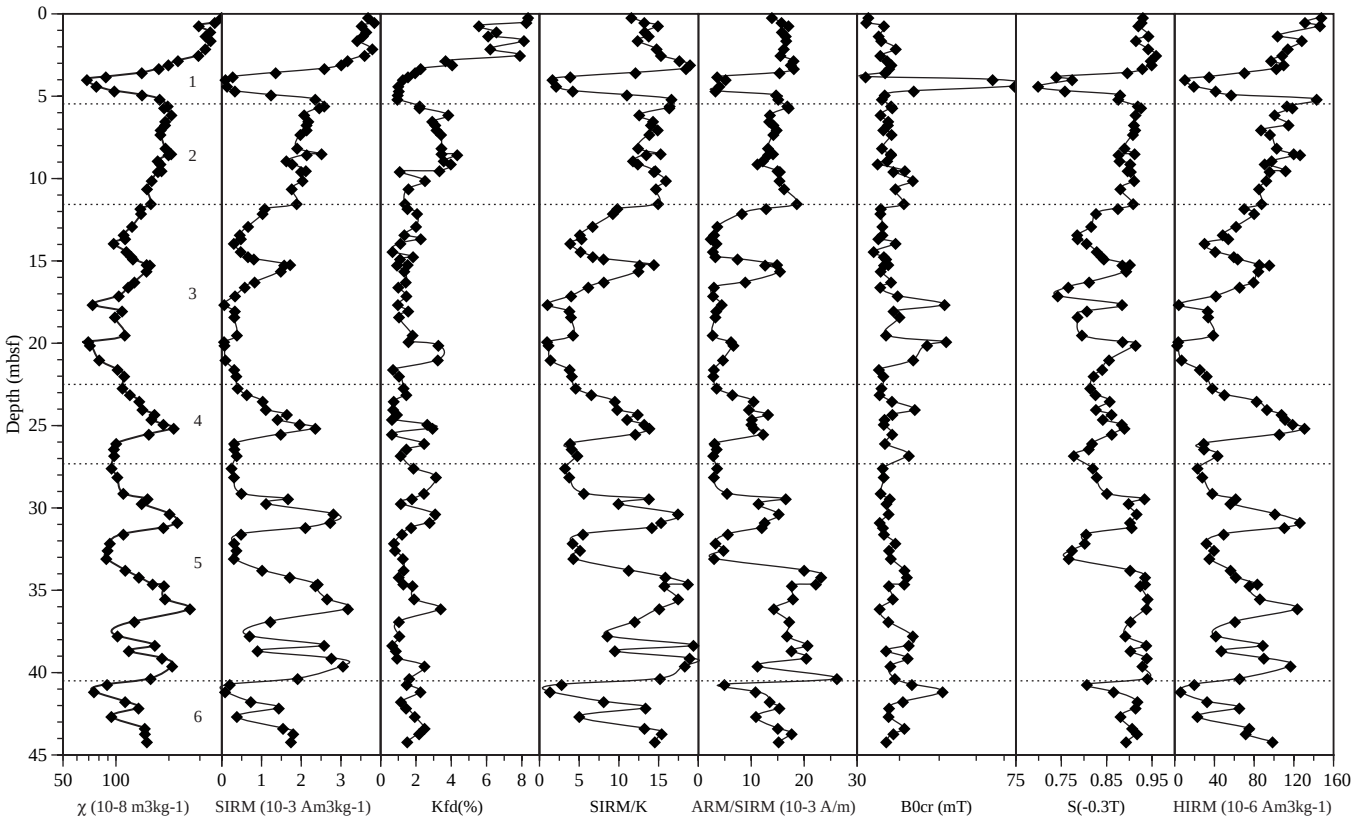

Figure 9. Downcore variations of magnetic parameters and interparametric ratios measured on samples from Site 976. Dashed lines = oxygen-isotope boundaries.

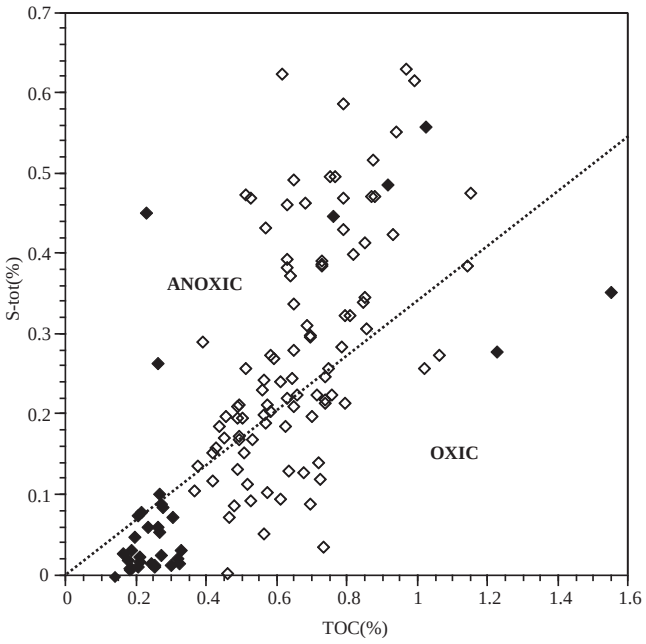

Figure 10. TOC vs. total S for Sites 975 (solid symbol) and 976 (open symbol). The distinction between oxic and anoxic environment (C/S = 2.8) is correlated to Quaternary normal marine, fine-grained detrital sediments (Berner, 1984).

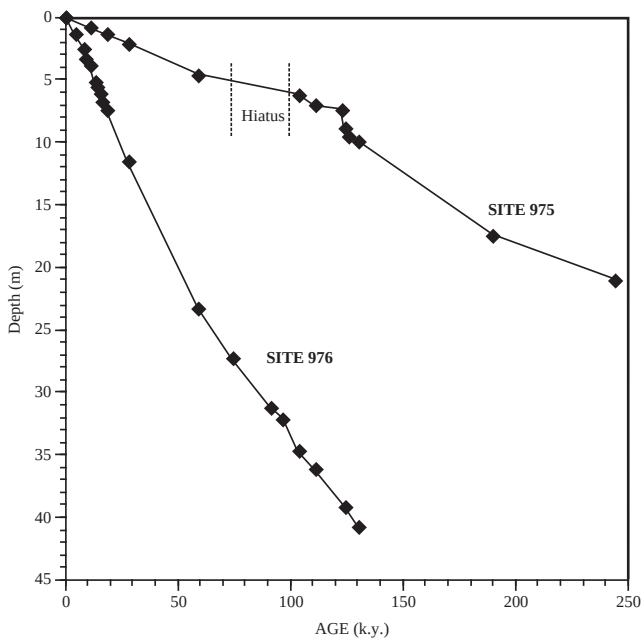

Figure 11. Sedimentation rates for Sites 975 and 976. Points used in the plots are reported in Tables 3 (Site 975) and 4 (Site 976).

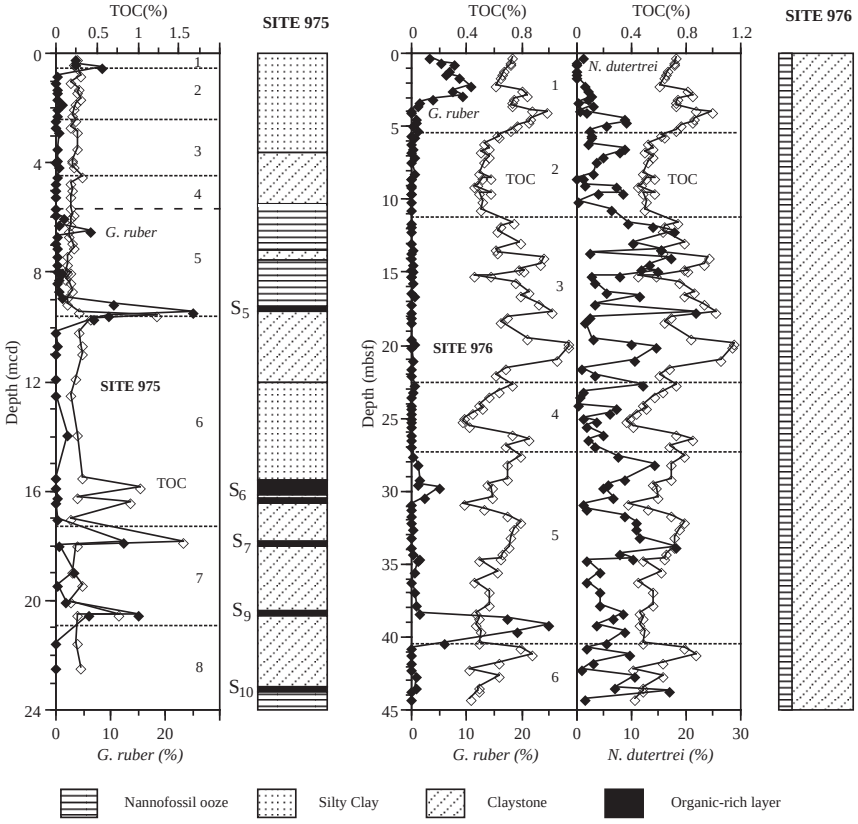

Figure 12. Down-core variations of TOC values and distribution of planktonic foraminifers considered to be sapropel indicators at Site 975 and 976.

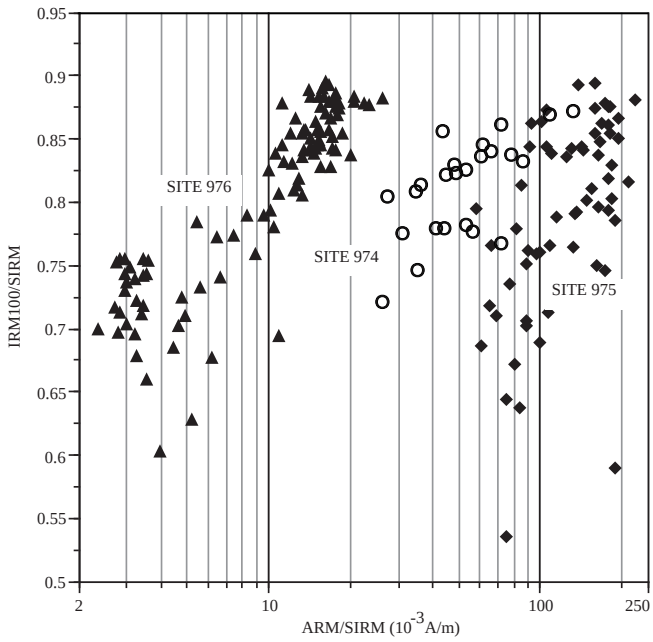

Figure 13. Interparametric ratio ARM/SIRM (SSD grain-size indicator) plotted against IRM_{100}/SIRM (indicative of magnetic mineralogy) for Sites 974, 975, and 976. Open circles = Site 974, solid squares = Site 975, and solid triangles = Site 976.

Paleoclimatic Record

The quantitative planktonic distribution allows one to reconstruct a detailed paleoclimatic trend for the western Mediterranean during the late Quaternary. The microfaunal assemblage at both Sites 975 and 976 document the presence of the Holocene in the uppermost interval. At Site 976, which is characterized by a quite high sedimentation rate, the abundance at the top of the core of *G. bulloides* and *G. inflata* suggests that it represents the present-day assemblages. In fact, at present, the Alboran Sea is characterized by the dominance of *G. inflata* during winter time (Deveaux, 1985) and by *G. bulloides* during summer season (Cifelli, 1974).

The reconstructed climatic trend is characterized by cold-temperate conditions with high values during the Holocene time and Eemian interval (oxygen-isotope substage 5e). The two oxygen-isotope boundaries 6/5 and 2/1 corresponding respectively to Termination II and I, are characterized by the same pattern: the passage between two extreme climatic conditions (cold and warm) is rapid and very well documented. At Site 975, a higher sedimentation rate during the Eemian substage (45cm/k.y.) documents a detailed paleoclimatic record. Significant fluctuations appear recorded during this time interval suggesting that it is divided into three substages, as also observed in North Atlantic cores by Fronval and Jansen (1996).

The paleoclimatic record shows a cyclicity that is also well recorded by magnetic parameters. This trend is similar to the rapid oxygen-isotope oscillations observed in the GRIP ice-core (Dansgaard et al., 1984). Several abrupt colder episodes are characterized by the dominance of cold species with a peak in frequency of *N. pachyderma* (left-coiling) and/or *G. quinqueloba*. This association, together

with the minimum in the number of planktonic foraminifers is exactly the same biological record observed in the Heinrich events documented in the North Atlantic sediments (Bond et al., 1993; Maslin et al., 1995). Some of these events can also be identified in the magnetic parameter profiles. All this evidence suggests that the oceanographic setting of Site 976 is strongly influenced by the water-mass exchange across the Gibraltar sill.

Occurrence of Sapropels in the Western Mediterranean

Sapropel layers were identified at both sites. At Site 975 the considered time interval includes sapropels S_1–S_9 in the Eastern Mediterranean Basin, and some of them have been identified within the cores. Most of these layers (S_5, S_6, S_7, S_9; Fig. 4) correspond to well-identified dark intervals with rock magnetic properties typical of anoxic environments. As discussed in the "Results" section, this chapter, the sapropels S_3 and S_4 belong to an interval that is missing in the sequence (Fig. 5).

At Site 976 the sapropel identification is not straightforward. Neither color nor organic-carbon content can be used as discriminant factors. No main changes occur in the sediment color and the organic-carbon profile exhibits several peaks scattered along the core. The site was anoxic during most of the time interval studied, and this makes it difficult to recognize the sapropels by using "anoxic features." The planktonic microfossil record has been the first and discriminant criteria for sapropel identification.

Several studies have shown that an unusual planktonic foraminiferal fauna characterizes the sapropel with peaks in frequencies of *G. ruber, G. bulloides, O. universa,* and, in many levels, of *N. dutertrei* (Cita et al., 1977; Vergnaud-Grazzini et al., 1977; Thunell and Lohmann, 1979; Muerdter and Kenneth, 1983/84). In most of these layers, the planktonic assemblage (abundance of *N. dutertrei)* and the oxygen-isotope depletion suggest that the surface-water salinity was relatively low (Cita et al., 1977; Vergnaud-Grazzini et al., 1977; Williams and Thunell, 1979; Muerdter, 1984; Tang and Stott, 1993). We have noted that it is possible to discriminate the sapropels on the basis of the quantitative and qualitative variations in planktonic foraminifer assemblage, either in warm or cold intervals. The sapropel layers deposited during warm intervals are characterized by peaks in frequencies of *G. ruber* and occurrence of *G. ruber* var. *rosea*, while abundance of *N. dutertrei* characterizes the sapropel layers deposited in cold intervals. This feature is also typical of the sediments from the western Mediterranean as shown in Figure 12. Both these species inhabit surface waters and are well documented in the literature to be related to low salinity (Bé and Tolderlund, 1971; Cita et al., 1977; Fairbanks et al., 1982; Rohling and Gieskes, 1989; Tang and Stott, 1993). Qualitative evidence shows the presence of several species with very thin tests and large pores, which can be easily detected even by optical microscope (see fig. 9 in Borsetti et al., 1995). Together with the presence of organic matter, which adheres to the test (as reported in fig. 7 of Cita et al., 1996) or pyritization processes, there are characteristic features of planktonic assemblages observed within sapropel layers found in the eastern Mediterranean Sea.

The high microfaunal commonality with the assemblage documented during the sapropel layer deposition in the Eastern Mediterranean Sea, combined with increasing organic-carbon content, magnetic measurements, and the stratigraphic position, support our interpretation.

The stratigraphic position of the recognized sapropel layers at Sites 975 and 976, together with the associated total organic carbon content, is listed in Tables 5 and 6. The estimated age for the recognized sapropel layers at both the sites 975 and 976 (reported in Tables 5 and 6) is in agreement with the age obtained by astronomical calibration for the same sapropels in the eastern Mediterranean (Lourens et al., 1996).

Table 5. Position, TOC value, and estimated and expected astronomical ages of the identified sapropel layers at Site 975.

Depth (mcd)	Sapropel	TOC (%)	Average age (k.y.)	Astronomical age (k.y.)
0.5	S_1	0.27	8.5	8
4.44	S_2	0.32	56	55
6.19	S_4	0.18	102	102
9.42	S_5	0.27	124	124
9.55	S_5	1.22		
15.81	S_{6a}	1.02	174	172
16.37	S_{6b}	0.91	178	
17.84	S_7	1.55	194	195
19.4	S_8	0.32	218	217
20.46	S_9	0.76	240	240

Note: Total organic carbon = wt% of whole sample. Ages are based on Lourens et al. (1996).

Table 6. Position, TOC value, and estimated and expected astronomical ages of the identified sapropel layers at Site 976.

Depth (mbsf)	Sapropel	TOC (%)	Average age (k.y.)	Astronomical age (k.y.)
2.50	S_1	0.81	8.5	8
2.82	S_1	0.85		
20.10	S_2	1.14	53	55
20.99	S_2	1.06		
29.42	S_3	0.55	82	81
33.05	S_4	0.72	102	102
33.76	S_4	0.71		
34.18	S_4	0.66		
38.65	S_5	0.49	123	124
39.10	S_5	0.46		

Note: Total organic carbon = wt% of whole sample. Ages are based on Lourens et al. (1996).

Finding sapropel layers in the western Mediterranean agrees with the oceanographic setting of the basin as shown by the presence of the Levantine Intermediate Water in the Gibraltar Sill (Loubere, 1987).

CONCLUSIONS

Planktonic foraminifers distribution and magnetic parameters integrated with geochemical analysis on sediments collected in the Western Mediterranean Sea document a paleoclimatic record that can be correlated with the trend recognized on a global scale for the last 140 k.y. The coherent pattern of different proxies suggests that they are dominated by the same factor—the climate.

The following conclusions can be drawn from our data:

1. The biological record corresponding to sapropel layers can be identified near the Gibraltar Strait, implying that the mechanism responsible for their deposition is not restricted to the eastern Mediterranean.
2. The sapropel layers yield a peculiar planktonic foraminiferal assemblage with high percentage of *G. ruber* and *N. dutertrei.*
3. High-resolution data show short-term climatic oscillations characterized by rapid cooling that can be correlated with the occurrence of Heinrich layers in the North Atlantic.
4. The Blake event has been identified in the Balearic Basin and appears constrained between about 119 and 123 ka.
5. Rock magnetic parameters show that different sources characterize the ferrimagnetic minerals from the Tyrrhenian sea, the Balearic Basin, and the Alboran Sea. The first exhibits the higher magnetic content, which is related to a possible volcanic source, whereas a bacterial and detrital source can be recognized at Sites 975 and 976.

6. Oscillations in the organic carbon content at Site 976 reflect variations in the primary productivity.
7. The high sedimentation rate observed at Site 976 provides a potential for high-resolution paleoclimatic investigations that can be compared with ice cores.

ACKNOWLEDGMENTS

The authors gratefully acknowledge the support of M.B. Cita who made possible this study. We are indebted to R. von Grafenstein, R. Zahn, N. Combourieu Nebout, and P. Belanger for many fruitful discussion and the use of their data. We also thank W. Landuzzi and G. Rovatti for laboratory assistance. C. Laj and L. Sagnotti helped to improve the manuscript by valuable comments. This is IGM publication No. 1100.

REFERENCES

Bé, A.W.H., and Tolderlund, D.S., 1971. Distribution and ecology of living planktonic foraminifera in surface waters of the Atlantic and Indian Oceans. *In* Funnel, B.M., and Riedel, W.R. (Eds.), *The Micropaleontology of Oceans:* Cambridge (Cambridge Univ. Press), 105–149.

Berner, R.A., 1984. Sedimentary pyrite formation: an update. *Geochim. Cosmochim. Acta,* 48:605–615.

Bloemendal, J., Lamb, B., and King, J., 1988. Paleoenvironmental implications of rock-magnetic properties of late Quaternary sediment cores from the eastern equatorial Atlantic. *Paleoceanography,* 3:61–87.

Bond, G., Broecker, W., Johnsen, S., McManus, J., Labeyrie, L., Jouzel, J., and Bonani, G., 1993. Correlations between climate records from the North Atlantic sediments and Greenland ice. *Nature,* 365:143–147.

Borsetti, A.M., Capotondi, L., Cati, F., Negri, A., Vergnaud-Grazzini, C., Alberini, C., Colantoni, P., and Curzi, P., 1995. Biostratigraphic events and late quaternary tectonics in the Dosso Gallignani (Central-Southern Adriatic Sea). *G. Geol.*, 57:41–58.

Calvert, S.E., 1983. Geochemistry of Pleistocene sapropels and associated sediments from the Eastern Mediterranean. *Oceanol. Acta,* 6:225–267.

Canfield, D.E., and Berner, R.A., 1987. Dissolution and pyritization of magnetite in anoxic marine sediments. *Geochim. Cosmochim. Acta,* 51:645–659.

Capotondi, L., Borsetti, A.M., and Asioli, A., 1994. Ecozonazione a Foraminiferi planctonici e paleoceanografia dell'ultima deglaciazione nel Mediterraneo centale. *Atti X Conv. AIOL,* 107–115.

Capotondi, L., Borsetti, A.M., and Vergnaud-Grazzini, C., 1987. Bioestratigraphie et composition isotopique de Foraminifères planctiques des derniers 140000 ans dans la région de Minorque (Méditerranèe occidentale). *C. R. Acad. Sci. Ser. 2,* 305:493–498.

Cifelli, R., 1974. Planktonic foraminifer from the Mediterranean and adjacent Atlantic waters (Cruise 49 of the Atlantic II, 1969). *J. Foraminifer. Res.*, 4:171–183.

Cita, M.B., Broglia, C., Malinverno, A., Spezzibottiani, G., Tomadin, L., and Violanti, D., 1982. Late Quaternary pelagic sedimentation on the southern Calabrian Ridge and western Mediterranean Ridge, Eastern Mediterranean. *Mar. Micropaleontol.*, 7:135–162.

Cita, M.B., Erba, E., Lucchi, R., Pott, M., van der Meer, R., and Nieto, L., 1996. Stratigraphy and sedimentation in the Mediterranean Ridge diapiric belt. *Mar. Geol.*, 132:131–150.

Cita, M.B., and Grignani, D., 1982. Nature and origin of Late Neogene Mediterranean sapropels. *In* Schlanger, S.O., and Cita, M.B. (Eds.), *Nature and Origin of Cretaceous Carbon-rich Facies:* London (Academic Press), 165–196.

Cita, M.B., Vergnaud-Grazzini, C., Robert, C., Chamley, H., Ciaranfi, N., and D'Onofrio, S., 1977. Paleoclimatic record of a long deep sea core from the eastern Mediterranean. *Quat. Res.*, 8:205–235.

Comas, M.C., Zahn, R., Klaus, A., et al., 1996. *Proc. ODP, Init. Repts.*, 161: College Station, TX (Ocean Drilling Program).

Dansgaard, W., Johnsen, S.J., Clausen, H.B., Dahl-Jensen, N., Gundestrup, N., and Hammer, C.U., 1984. North Atlantic climatic oscillations revealed by deep Greenland ice cores. *In* Hansen, J.E., and Takahashi, T. (Eds.), *Climate Processes and Climate Sensitivity.* Geophys. Monogr., 29:288–298.

Dansgaard, W., Johnsen, S.J., Clausen, H.B., Dahl-Jensen, D., Gundestrup, N.S., Hammer, C.U., Hvidberg, C.S., Steffensen, J.P., Sveinbjörnsdottir, A.E., Jouzel, J., and Bond, G., 1993. Evidence for general instability of past climate from a 250-kyr ice-core record. *Nature,* 364:218–220.

De Castro Coppa, M.G., Montcharmont Zei, M., Placella, B., Sgarella, F., and Taddei Ruggiero, E., 1980. Distribuzione stagionale e verticale dei Foraminiferi planctonici del Golfo di Napoli. *Boll. Soc. Nat.*, 89:1–25.

Deveaux, M., 1985. Foraminiferes et isotopes legers: indicateurs stratigraphiques et environmentaux de la derniere deglaciation quaternaire, Golfe de Cadix-Mer d'Alboran [Thesis]. Univ. Bordeaux.

Doh, S.-J., King, J.W., and Leinen, M., 1988. A rock-magnetic study of giant piston core LL4-GPC3 from the central North Pacific and its paleoceanographic implications. *Paleoceanography,* 3:89–111.

Emeis, K.-C., Camerlenghi, A., McKenzie, J.A., Rio, D., and Sprovieri, R., 1991. The occurrence and significance of Pleistocene and Upper Pliocene sapropels in the Tyrrhenian Sea. *Mar. Geol.*, 100:155–182.

Fairbanks, R.G., Sverdlove, M., Free, R., Wiebe, P.H., and Bé, A.W.H., 1982. Vertical distribution and isotopic fractionation of living planktonic foraminifera from the Panama Basin. *Nature,* 298:841–844.

Fang, X.M., Li, J.J., Van der Voo, R., MacNiocaill, C., Dai, X.R., Kemp, R.A., Derbyshire, E., Cao, J.X., Wang, J.M., and Wang, G., 1997. A record of the Blake Event during the last interglacial paleosol in the western Loess Plateau of China. *Earth Planet. Sci. Lett.*, 146:73–82.

Fronval, T., and Jansen, E., 1996. Rapid changes in ocean circulation and heat flux in the Nordic seas during the last interglacial period. *Nature,* 383:806–810.

Hilgen, F.J., 1991. Astronomical calibration of Gauss to Matuyama sapropels in the Mediterranean and implication for the geomagnetic polarity time scale. *Earth Planet. Sci. Lett.*, 104:226–244.

Imbrie, J., Hays, J.D., Martinson, D.G., McIntyre, A., Mix, A.C., Morley, J.J., Pisias, N.G., Prell, W.L., and Shackleton, N.J., 1984. The orbital theory of Pleistocene climate: support from a revised chronology of the marine $\delta^{18}O$ record. *In* Berger, A., Imbrie, J., Hays, J., Kukla, G., and Saltzman, B. (Eds.), *Milankovitch and Climate* (Pt. 1), NATO ASI Ser. C, Math Phys. Sci., 126:269–305.

Karlin, R., 1990. Magnetite mineral diagenesis in suboxic sediments at Bettis Site W-N, NE Pacific Ocean. *J. Geophys. Res.*, 95:4421–4436.

Karlin, R., and Levi, S., 1983. Diagenesis of magnetic minerals in recent hemipelagic sediments. *Nature,* 303:327–330.

Kent, D.V., 1982. Apparent correlation of paleomagnetic intensity and climatic records in deep-sea sediments. *Nature,* 299:538–539.

Kidd, R.B., Cita, M.B., and Ryan, W.B.F., 1978. Stratigraphy of eastern Mediterranean sapropel sequences recovered during DSDP Leg 42A and their paleoenvironmental significance. *In* Hsü, K.J., Montadert, L., et al., *Init. Repts. DSDP,* 42 (Pt. 1): Washington (U.S. Govt. Printing Office), 421–443.

Leventhal, J.S., 1983. An interpretation of carbon and sulfur relationships in Black Sea sediments as indicators of environments of deposition. *Geochim. Cosmochim. Acta,* 47:133–137.

Loubere, P., 1987. Changes in mid-depth North Atlantic and Mediterranean circulation during the late Pliocene—isotopic and sedimentological evidence. *Mar. Geol.*, 77:15–38.

Lourens, L.J., Antonarakou, A., Hilgen, F.J., Van Hoof, A.A.M., Vergnaud-Grazzini, C., and Zachariasse, W.J., 1996. Evaluation of the Plio-Pleistocene astronomical timescale. *Paleoceanography,* 11:391–413.

Martinson, D.G., Pisias, N.G., Hays, J.D., Imbrie, J., Moore, T.C., Jr., and Shackleton, N.J., 1987. Age dating and the orbital theory of the ice ages: development of a high-resolution 0 to 300,000-year chronostratigraphy. *Quat. Res.*, 27:1–29.

Maslin, M.A., Shackleton, N., and Pflaumann, U., 1995. Surface water temperature, salinity and density changes in the N.E. Atlantic during the last 45,000 years: Heinrich events, deep water formation and climatic rebounds. *Paleoceanography,* 10:527–544.

McCoy, F.W., and Cornell, W., 1990. Volcaniclastic sediments in the Tyrrhenian Basin. *In* Kastens, K.A., Mascle, J., et al., *Proc. ODP, Sci. Results,* 107: College Station, TX (Ocean Drilling Program), 291–305.

McIver, R.D., 1975. Hydrocarbon occurrences from JOIDES Deep Sea Drilling Project. *Proc. Ninth Petrol. Congr.*, 269–280.

Muerdter, D.R., 1984. Low-salinity surface water incursions across the Strait of Sicily during late Quaternary sapropel intervals. *Mar. Geol.*, 58:401–414.

Muerdter, D.R., and Kennett, J.P., 1983/84. Late Quaternary planktonic foraminiferal biostratigraphy, Strait of Sicily, Mediterranean Sea. *Mar. Micropaleontol.*, 8:339–359.

Muerdter, D.R., Kennett, J.P., and Thunell, R.C., 1984. Late Quaternary sapropel sediments in the eastern Mediterranean Sea: faunal variations and chronology. *Quat. Res.*, 21:385–403.

Nowaczyk, N.R., Frederichs, T.W., and Gard, G., 1994. Magnetostratigraphic data from late Quaternary sediments from the Yermak Plateau. Arctic ocean: evidence for four geomagnetic polarity events within the last 170 ka of the Brunhes chron. *Geophys. J. Int.*, 117:453–471.

Olausson, E., 1961. Studies of deep-sea cores. *Rep. Swed. Deep-Sea Exped., 1947–1948*, 8:335–391.

Oldfield, F., 1994. Toward the discrimination of fine-grained ferrimagnets by magnetic measurements in lake and near-shore marine sediments. *J. Geophys. Res.*, 99:9045–9050.

Oldfield, F., and Robinson, S.G., 1985. Geomagnetism and palaeoclimate. *In* Tooley, M.J., and Sheail, G.M. (Eds.), *The Climatic Scene:* London (Allen and Unwin), 186–205.

Pujol, C., and Vergnaud-Grazzini, C., 1989. Palaeoceanography of the Last Deglaciation in the Alboran Sea (Western Mediterranean): stable isotope and planktonic foraminiferal records. *Mar. Micropaleontol.*, 15:153–179.

————, 1995. Distribution patterns of live planktic foraminifers as related to regional hydrography and productive systems of the Mediterranean Sea. *Mar. Micropaleontol.*, 25:187–217.

Robinson, S.G., 1986. The late Pleistocene paleoclimatic record of North Atlantic deep-sea sediments revealed by mineral-magnetic measurements. *Phys. Earth Planet. Inter.*, 42:22–47.

Robinson, S.G., Maslin, M.A., and McCave, I.N., 1995. Magnetic susceptibility variations in late Pleistocene deep-sea sediments of the N.E. Atlantic: implications for ice-rafting and paleocirculation at the last glacial maximum. *Paleoceanography*, 10:221-250.

Rohling, E.J., and Gieskes, W.W.C., 1989. Late Quaternary changes in Mediterranean intermediate water density and formation rate. *Paleoceanography*, 4:531–545.

Rossignol-Strick, M., 1983. African monsoons: an immediate climate response to orbital insolation. *Nature*, 304:46–49.

————, 1985. Mediterranean Quaternary sapropels, an immediate response of the African Monsoon to variation of insolation. *Palaeogeogr., Palaeoclimatol., Palaeoecol.*, 49:237–263.

Stein, R., 1990. Organic carbon/sedimentation rate relationship and its paleoenvironmental significance for marine sediments. *Geo-Mar. Lett.*, 10:37–44.

————, 1991. *Accumulation of Organic Carbon in Marine Sediments: Results from the Deep Sea Drilling Project/Ocean Drilling Program (DSDP/ODP).* Lect. Notes Earth Sci., 34: Heidelberg (Springer-Verlag).

Tang, C.M., and Stott, L.D., 1993. Seasonal salinity changes during Mediterranean sapropel deposition 9000 years B.P.: evidence from isotopic analyses of individual planktonic foraminifera. *Paleoceanography*, 8:473–493.

Tarduno, J.A., and Wilkison, S.L., 1996. Non-steady state magnetic mineral reduction, chemical lock-in, and delayed remanence acquisition in pelagic sediments. *Earth Planet. Sci. Lett.*, 144:315–326.

Thunell, R., Williams, D.F., and Kennett, J.P., 1977. Late Quaternary paleoclimatology, stratigraphy and sapropel history in Eastern mediterranean deep-sea sediments. *Mar. Micropaleontol.*, 2:371–388.

Thunell, R.C., 1978. Distribution of planktonic foraminifera in surface sediments of the Mediterranean Sea. *Mar. Micropaleontol.*, 3:147–173.

————, 1979. Pliocene-Pleistocene paleotemperature and paleosalinity history of the Mediterranean Sea: results from Deep Sea Drilling Project Sites 125 and 132. *Mar. Micropaleontol.*, 4:173–187.

Thunell, R.C., and Lohmann, G.P., 1979. Planktonic foraminiferal fauna associated with eastern Mediterranean quaternary stagnations. *Nature*, 281:211–213.

Thunell, R.C., Williams, D.F., Tappa, E., Rio, D., and Raffi, I., 1990. Pliocene-Pleistocene stable isotope record for ODP Site 653, Tyrrhenian Basin: implications for paleoenvironmental history of the Mediterranean Sea. *In* Kastens, K.A., Mascle, J., et al., *Proc. ODP, Sci. Results*, 107: College Station, TX (Ocean Drilling Program), 387–399.

Tucholka, P., Fontugue, M., Guichard, F., and Paterne, M., 1987. The Blake polarity episode in cores from the Mediterranean Sea. *Earth Planet. Sci. Lett.*, 86:320–326.

Vergnaud-Grazzini, C., Ryan, W.B.F., and Cita, M.B., 1977. Stable isotope fractionation, climatic change and episodic stagnation in the Eastern Mediterranean during the Late Quaternary. *Mar. Micropaleontol.*, 2:353–370.

Vergnaud Grazzini, C., Saliège, J.F., Urrutiaguer, M.J., and Iannace, A., 1990. Oxygen and carbon isotope stratigraphy of ODP Hole 653A and Site 654: the Pliocene-Pleistocene glacial history recorded in the Tyrrhenian Basin (West Mediterranean). *In* Kastens, K.A., Mascle, J., et al., *Proc. ODP, Sci. Results*, 107: College Station, TX (Ocean Drilling Program), 361–386.

Vigliotti, L., 1997. Magnetic properties of light and dark sediment layers from the Japan Sea: diagenetic and paleoclimatic implications. *Quat. Sci. Rev.*, 16:10:1–21.

Williams, D.F., and Thunell, R.C., 1979. Faunal and oxygen isotopic evidence for surface water salinity changes during sapropel formation in the eastern Mediterranean. *Sediment. Geol.*, 23:81–93.

Woillard, G.M., 1978. Gran Pile Peat Bog: a continuous pollen record for the last 140,000 years. *Quat. Res.*, 9:1–21.

Date of initial receipt: 16 May 1997
Date of acceptance: 16 December 1997
Ms 161SR-243